Post-seismic crustal deformation and strain rate in Bhuj region, western India, after the 2001 January 26 earthquake

C. D. Reddy and P. S. Sunil

Indian Institute of Geomagnetism, New Panvel, Navi Mumbai – 410218, India. E-mail: cdreddy@iigs.iigm.res.in

SUMMARY

The M_w 7.6 Bhuj earthquake in Gujarat, western India, which occurred on 2001 January 26 was a major intraplate event in the Indian subcontinent. To study the characteristics of transient post-seismic deformation at the earth's surface, to elucidate the distribution of strain accumulation rate and so understand the earthquake recurrence process, five GPS campaigns were conducted at 14 sites, in Bhuj region during 2001–2002. The daily variations in the site position coordinates and the baselines during the early after-shock period (i.e. for 21 d starting from 2001 February 10–March 2) showed no short-term post-seismic crustal deformation. Neither logarithmic nor exponential function could be well fitted to any of the components of the time-series of the position co-coordinates, indicating no discernable contribution from viscoelastic relaxation, poroelastic rebound or afterslip mechanisms.

The estimated velocity field in ITRF2000 spanning five epochs during 2001–2002 has an average of 50 mm yr^{-1} in north–northeast direction. To obtain a better perspective of post-seismic deformation in the epicentral track, the residual velocity field has been expressed in an India fixed reference frame. The residual velocity of 11.62 mm yr^{-1} in a north–northwest direction and 5.24 mm yr^{-1} towards the south seen at sites south and north of the epicentre, respectively, indicates localized ongoing convergence in the epicentral region. At sites away from the epicentre no significant deformation took place. The estimated principal strain from the velocity field gives average compression and extension rates of 0.07 and 0.04 micro-strain yr^{-1}, respectively. A zone of maximum compressive strain rate of 0.30 micro-strain yr^{-1} with azimuth of 11° delineated north of the epicentral region shows good agreement with seismic deformation along the blind fault derived from earthquake focal mechanisms. These results suggest ongoing transpressional deformation across the area with a blocked structure embedded between the North Wagad Fault and South Wagad Fault. This deformation may be related to the present neo-tectonic compressive stress regime of the Indian Plate due to its NNE movement against the collision front in the north and its proximity to the triple junction in the western continental margin of the study area.

Key words: Satellite geodesy; Transient deformation; Intra-plate processes; High strain; deformation zones.

GJI Seismology

1 INTRODUCTION

The surface of the earth is continuously strained by tectonic processes and monitoring surface deformation is essential for quantitative understanding of the seismo-tectonics. Furthermore, relaxation of the perturbed stresses following an earthquake causes post-seismic crustal deformation. Continuous monitoring of post-seismic deformation facilitates improved understanding of the physics of relaxation of stress perturbation, viscous rheology and modelling the crustal dynamics of a region. The strain rate distribution helps in evaluating the seismic risk and to infer the causative tectonic forces. The Bhuj earthquake on 2001 January 26 provides a unique opportunity to study these aspects in an intraplate setting.

Kutch province, which includes the Bhuj region, is a major seismogenic domain in western India (Fig. 1) and forms a crucial geodynamic part of the western continental margin of the Indian subcontinent. This region is seismically categorized under active zone 5 (Arya 2000) of the Indian subcontinent and extends 250 km in east–west direction and 150 km in north–south direction. The Kutch basin can be distinguished by major fault systems (Malik *et al.* 2000; Karant 2001; Biswas & Khattri 2002) including the Nagar Parkar Fault (NPF) and Allah Bund Fault (ABF) (formed during the $M \approx 7.8$, 1819 earthquake) in the northern region (Bilham 1999; Rajendran & Rajendran 2001) and the Kutch Mainland Fault (KMF) and Katrol Hill Fault (KHF) along which the 1956 earthquake occurred (Biswas 1987; Chung & Gao 1995) in the southern part of the basin. The northwest–southeast oriented Vigodi Fault and Banni
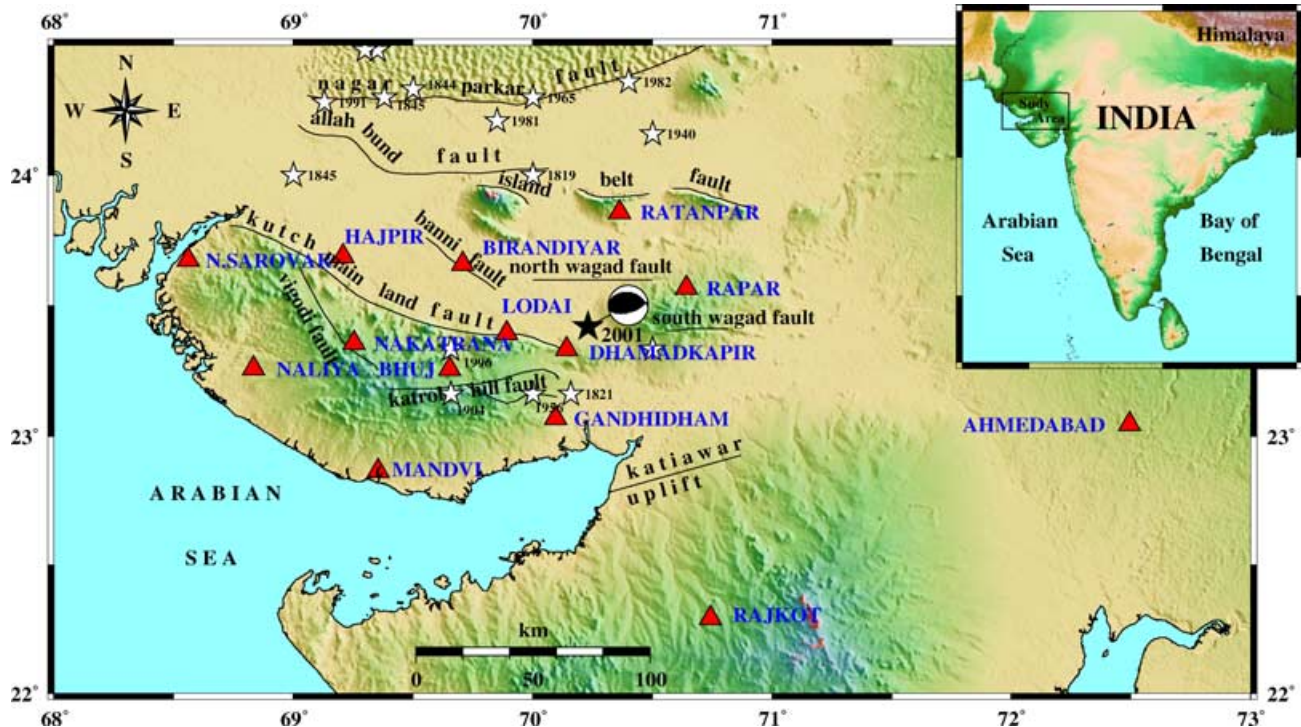
Figure 1. Tectonic map of Bhuj region with GPS locations (triangles) used for the present study. The black star indicates the epicentre location of 2001 earthquake with focal mechanism solution. White stars indicate the major earthquake epicentres occurred during past and black lines are major faults/lineaments. The rectangle in the inset represents the study area.

Fault and EW oriented North Wagad Fault (NWF) and South Wagad Fault (SWF) (Mandal *et al.* 2004) are also located from west to east of the Kutch rift basin, respectively. As shown in Fig. 1, most of the GPS sites installed for the present study fall in the vicinity of these faults.

Fig. 1 also shows the spatio-temporal distribution of historical earthquakes along with the 2001 earthquake location against the major tectonic elements given in the background. Damaging earthquakes occurred in 1845, 1856, 1864, 1903, 1927 and 1940. Before the 2001 earthquake, the last damaging earthquake in this region was the M_w 6 Anjar earthquake of 1956 that originated at a focal depth of 15 km. The 2001 January 26 Bhuj earthquake is considered to be the second largest and most deadly earthquake to have occurred in this region in recorded history (Bendick *et al.* 2001). Thus, this region has a history of a high frequency of damaging earthquakes having a low regional *b*-value indicating high stress. Biswas & Khattri (2002) provide a detailed description of the seismo-tectonics of the Bhuj earthquake prone region.

After the devastating earthquake on 2001 January 26 with M_w 7.6, the Kutch region became the focus of increased geophysical investigations. As a part of the Department of Science and Technology (DST), Government of India sponsored projects, various geophysical investigations were carried out. IIG Working Group (2001) published some of the details of these studies. To measure the post-seismic crustal deformation, and to investigate its mechanism, GPS observations around the source region have been made. We present results pertaining to five GPS campaigns made with 6–7 months interval during 2001–2002.

2 GPS DATA ANALYSIS

Dual frequency geodetic GPS receivers were used at 14 sites (shown in Fig. 1) in campaign mode. At each site, a minimum 48–72 hr of

GPS data were collected with a sampling interval of 30 s and an elevation mask of 15°. The GPS data were organized into 24 hr segments covering a UTC day to facilitate the integration of data from nine surrounding International GNSS Service (IGS) sites viz. Bangalore (IISC), Bahrain (BAHR), Degartia (DGAR), Kitab (KIT3), Kunming (KUNM), Nanyang (NTUS), Maldives (MALD), Poligan (POL2) and Urumgi (URUM). These sites were used to constrain the site coordinates in the study region. The data were processed with the GAMIT software (King & Bock 2000) to produce estimates and associated covariance matrix of station positions for each session with loose constraints on the parameters. To get a combined solution (site positions and velocities), all such covariance matrices are used as input to the GLOBK software (Herring 2000), which is a Kalman filter. The basic algorithms and a description of this technique are given in Herring *et al.* (1990). We estimated the station repeatabilities to provide an estimate of the precision of the measurements by combining the daily loosely constrained estimates of station coordinates and global h-files from Scripps Orbit and Permanent Array Centre (SOPAC).

The velocity vectors at each site in the well-determined International Terrestrial Reference Frame (ITRF2000) (Altamimi *et al.* 2002) have been obtained from these combined quasi-observations (Dong *et al.* 1998; McClusky *et al.* 2000). These ITRF2000 velocity solutions are useful for comparing/combining our results with other analyses since they are robustly tied to a conventionally defined reference frame. The 1σ uncertainties were derived by scaling the formal errors by the square root of chi-square per degree of freedom of the solution after reweighing the data from each campaign or monthly averaged SOPAC solution; such that their chi-square contributions were nearly equal (Chen *et al.* 2000). The velocity of our GPS sites relative to the Indian Plate were obtained by subtracting a recently determined geodetic rotation pole for the Indian Plate (determined from GPS stations relative to ITRF2000) from

Table 1. GPS stations (Stns.) velocities (Vel.) and 1σ uncertainties. Latitude (Lati.) and Longitude (Long.) are given in degrees with and number of GPS campaign occupation (Occu.) at each site. North and east velocities and uncertainties with reference to ITRF2000 and India fixed reference frame are given in mm yr^{-1}.

| Stns. | Lati. | Long. | Occu. | ITRF2000 | | | | India fixed | | | |
				N Vel.	N σ	E Vel.	E σ	N Vel.	N σ	E Vel.	E σ
AHMD	23.044	72.495	5	28.40	0.40	39.60	0.96	−2.531	0.40	1.265	0.96
RAJK	22.292	70.744	5	35.75	0.42	42.94	0.99	1.933	0.42	2.747	0.99
RAPR	23.568	70.644	5	33.19	0.59	38.48	1.37	−0.619	0.59	1.761	1.37
RATN	23.860	70.363	5	28.60	0.67	35.82	1.55	−5.188	0.67	−0.726	1.55
DHAM	23.332	70.143	5	44.64	0.60	32.58	1.39	10.870	0.60	−4.107	1.39
GAND	23.069	70.095	5	37.90	0.61	34.57	1.38	4.134	0.61	−2.201	1.38
LODA	23.394	69.892	5	32.88	0.81	31.76	1.82	−0.870	0.81	−4.845	1.82
BIRN	23.662	69.707	5	31.17	0.80	34.94	1.77	−2.564	0.80	−1.523	1.77
BHUJ	23.254	69.654	5	34.48	0.70	39.30	1.70	0.750	0.70	2.699	1.70
MAND	22.834	69.354	5	36.93	0.64	41.02	1.39	3.226	0.64	4.334	1.39
NAKA	23.355	69.255	5	33.32	0.69	35.68	1.58	−0.375	0.69	−0.791	1.58
HAJP	23.690	69.207	5	32.07	0.76	34.83	1.70	−1.621	0.76	−1.504	1.70
NALI	23.257	68.835	5	32.25	0.74	34.26	1.49	−1.407	0.74	−2.150	1.49
NARA	23.677	68.541	5	34.41	0.66	35.39	1.40	0.781	0.66	−0.792	1.40
IISC	13.021	77.570	5	32.18	0.37	41.17	0.41	−1.902	0.37	0.355	0.41

the estimated GPS velocity field (Socquet *et al.* 2006). In Table 1, Figs 4 and 6, we present the velocities of our GPS stations together with IGS station IISC (within the Indian Plate) with reference to ITRF2000 and in the India fixed reference frame, respectively. To compute the principal strain rate from the velocity field, we estimate the velocity gradient tensor across a Delaunay triangular mesh to provide the spatial variability of the strain rate pattern on a regular grid size. We computed the principal strain tensor at each gridpoint, using a common least-square procedure (Feigl *et al.* 1990) and taking into account the direction of principal strain axes, we derived the corresponding rates of shortening and elongation.

3 POST-SEISMIC DEFORMATION

To monitor the short-term post-seismic deformation associated with the Bhuj earthquake, the site coordinates and baselines were computed every day during 2001 February 10–March 2. As the surface deformation is expected to be accelerated immediately after the earthquake and there were many aftershocks during this time, the short-term post seismic deformation may be significant. We have attempted to determine realistic uncertainties for our daily variation in an iterative fashion and examined the time-series for all the stations by downweighting the daily solution for which the root-mean-square (rms) value is higher. Figs 2(a) and (b) show the time-series of the coordinates (in ITRF2000) in north–south (NS), east–west (EW) and up–down (UD) components at the sites Ahmedabad (AHMD), Rajkot (RAJK), Bhuj (BHUJ), Gandhidham (GAND), Mandvi (MAND), Lodai (LODA), Dhamadkapir (DHAM), Rapar (RAPR), Ratanpar (RATN), Naliya (NALI), Narayansarovar (NARA), Nakatrana (NAKA), Hajpir (HAJP) and Birandiyar (BIRN) with uncertainties ≤2 mm in north–south, ≤3 mm in east–west and ≤5 mm in up–down components. As the baseline vectors have the advantage of being unaffected by translation and rotation of reference frame and the satellite orbits, and form clear data set from which inference on deformation can be drawn more safely (Scherneck *et al.* 2001), selected baselines viz. bhuj-rapr and gand-ratn, which are cutting across the epicentral region (as shown in left and right lower most blocks in the Fig. 3) were estimated with uncertainties ≤2 and ≤5 mm in horizontal and vertical components, respectively. The time-series show that there was no detectable

short-term post-seismic deformation, during the initial 21 days of observation.

The continuation of the displacement time-series during 2001–2002 follow neither logarithmic nor exponential functions and as seen from the Figs 5(a) and (b), a linear trend fits well at all the sites. This indicates that there is no discernable post-seismic relaxation pertaining to either afterslip or/and viscoelastic mechanisms, else, it would have provided information on rheological properties of the lower crust and upper mantle (Pollitz 2003). Abundant and widespread coseismic liquefaction in the region suggests the possibility of poroelastic relaxation (Peltzer *et al.* 1998), but this could not be detected either. If any of the above mechanism/s extended to more than one year, it would have been reflected in the horizontal displacement time-series shown in Figs 5(a) and (b). However, lacking detailed pre-earthquake measurements of deformation in the region (Wallace *et al*. 2006) it is possible that the measured surface velocities are due to a very slowly decaying post-seismic process. Continued measurements over several more years should allow for resolution of this question.

We compared our results with the Miyagi earthquake (M_w 6.4) in northern Japan on 2003 July 26 and 1811–1812 New Madrid earthquakes (cumulative magnitude M_w = 7.5–8.3). No post-seismic displacement was detected associated with the Miyagi earthquake despite continuous data collected at three sites just above the source area (Miura *et al*. 2004). They suggest that the earthquakes of about M 6.5 do not accompany post-seismic deformation. Where as the post-seismic deformation associated with the New Madrid earthquakes represent long-term post-seismic process (Smalley *et al.* 2005). They speculate that any or a combination of poroelasticity decay, viscous relaxation and afterslip across the main rupture plane. Both the above earthquakes are intraplate type and the later is more similar to Bhuj earthquake. On the other hand, in Indian subcontinent, post-seismic deformation mechanism of 2005 October 8 Kashmir Earthquake (34.43N, 73.53E, 120 km WNW of Srinagar, ~1275 km north of Bhuj region) agree with characteristics of afterslip (Parsons *et al.* 2006; Reddy & Prajapati 2007). Finally, in the Andaman arc region, the post-seismic deformation portrays both afterslip and viscoelastic mechanism (Reddy *et al.* 2005; Pollitz *et al.* 2006). Here, we cannot compare Bhuj region with the above interpate earthquakes. Thus, as far as the post-seismic deformation
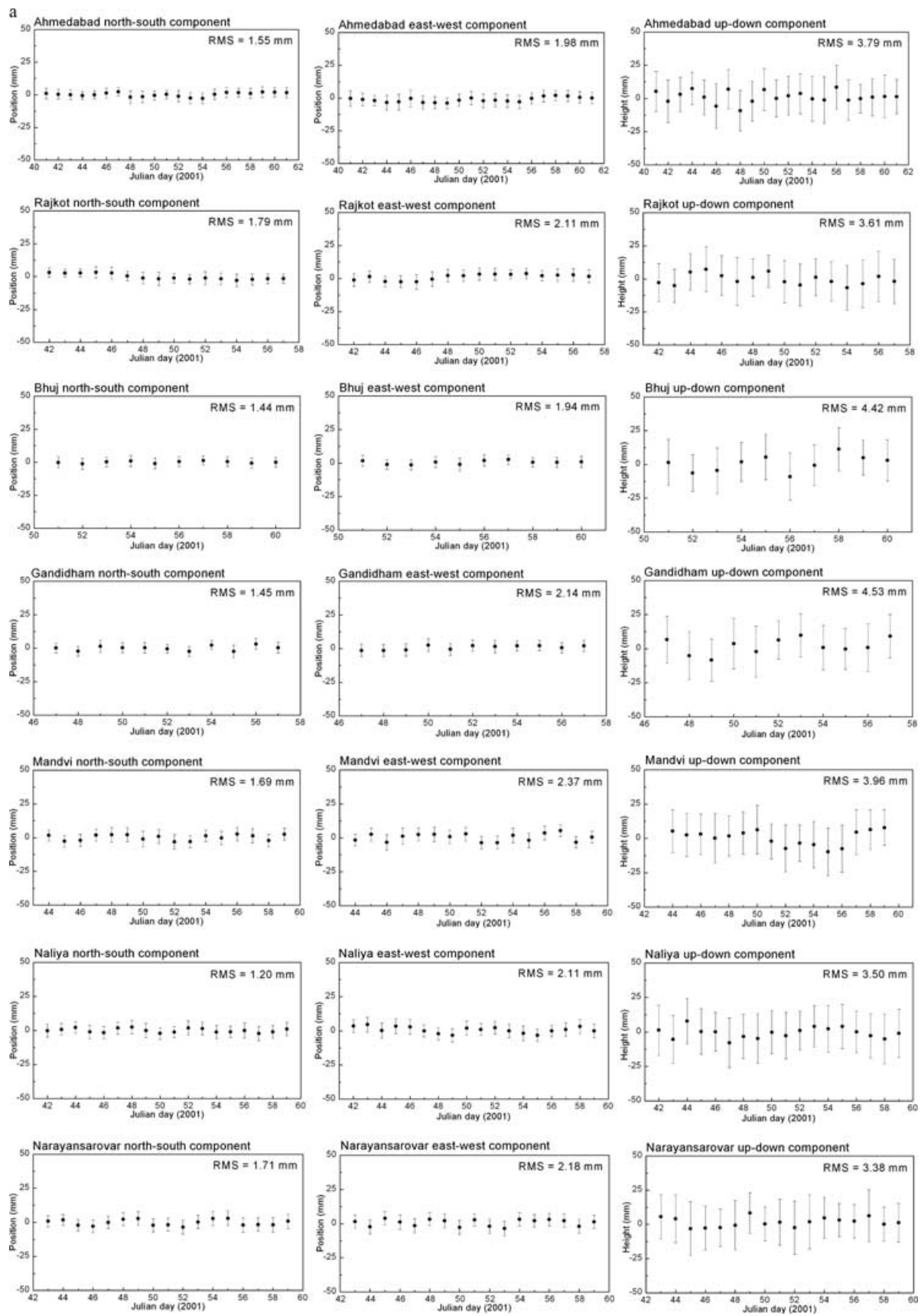
Figure 2. (a) Daily variability in position coordinates (NS, EW and vertical components) with rms value of repeatability estimated for 21 days (starting from 2001 February 10–March 2) at the sites AHMD, RAJK, BHUJ, GAND, MAND, NALI and NARA. (b). Daily variability in position coordinates (NS, EW and vertical components) with rms value of repeatability estimated for 21 days at the sites NAKA, LODA, DHAM, RAPR, RATN, BIRN and HAJP.
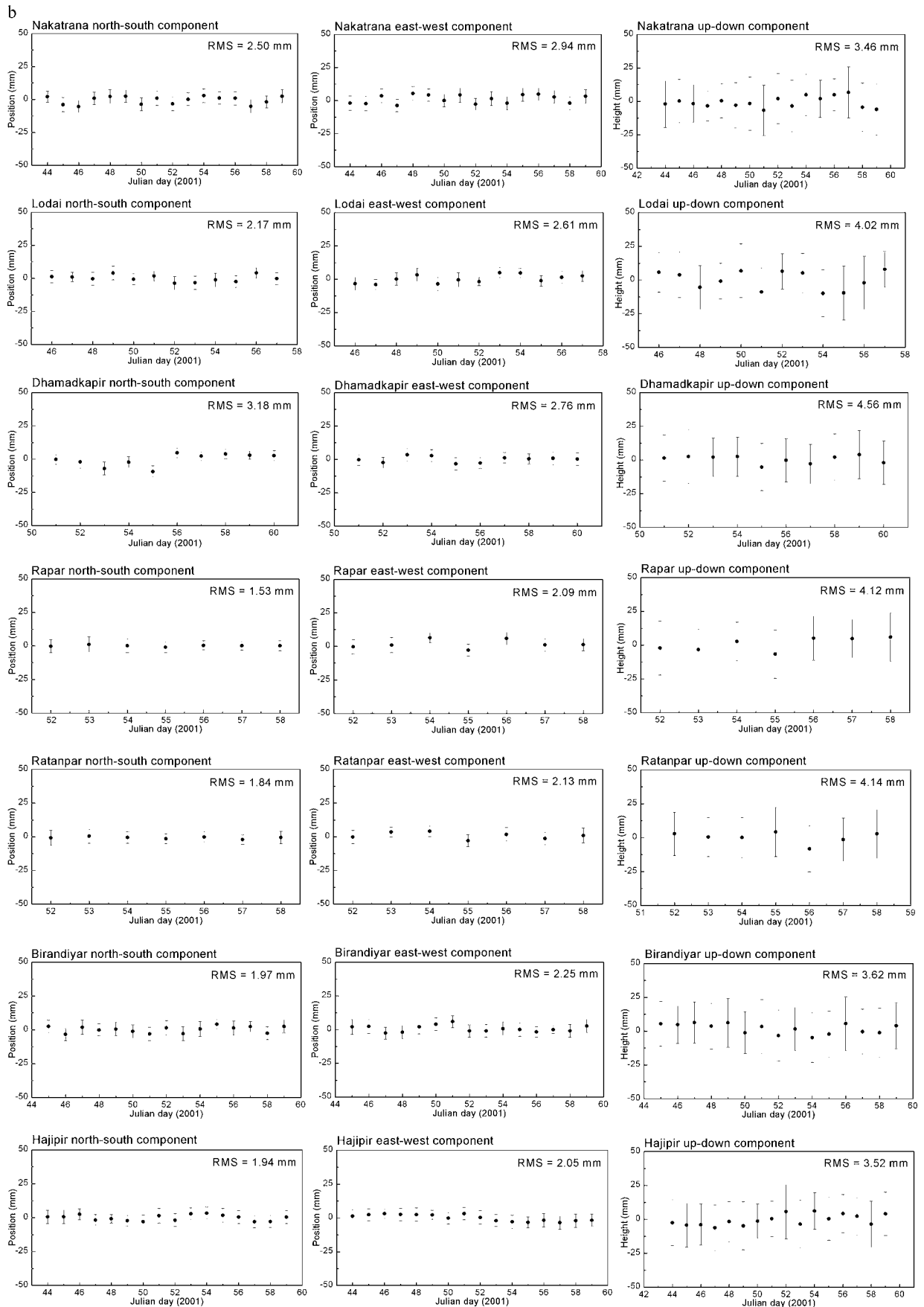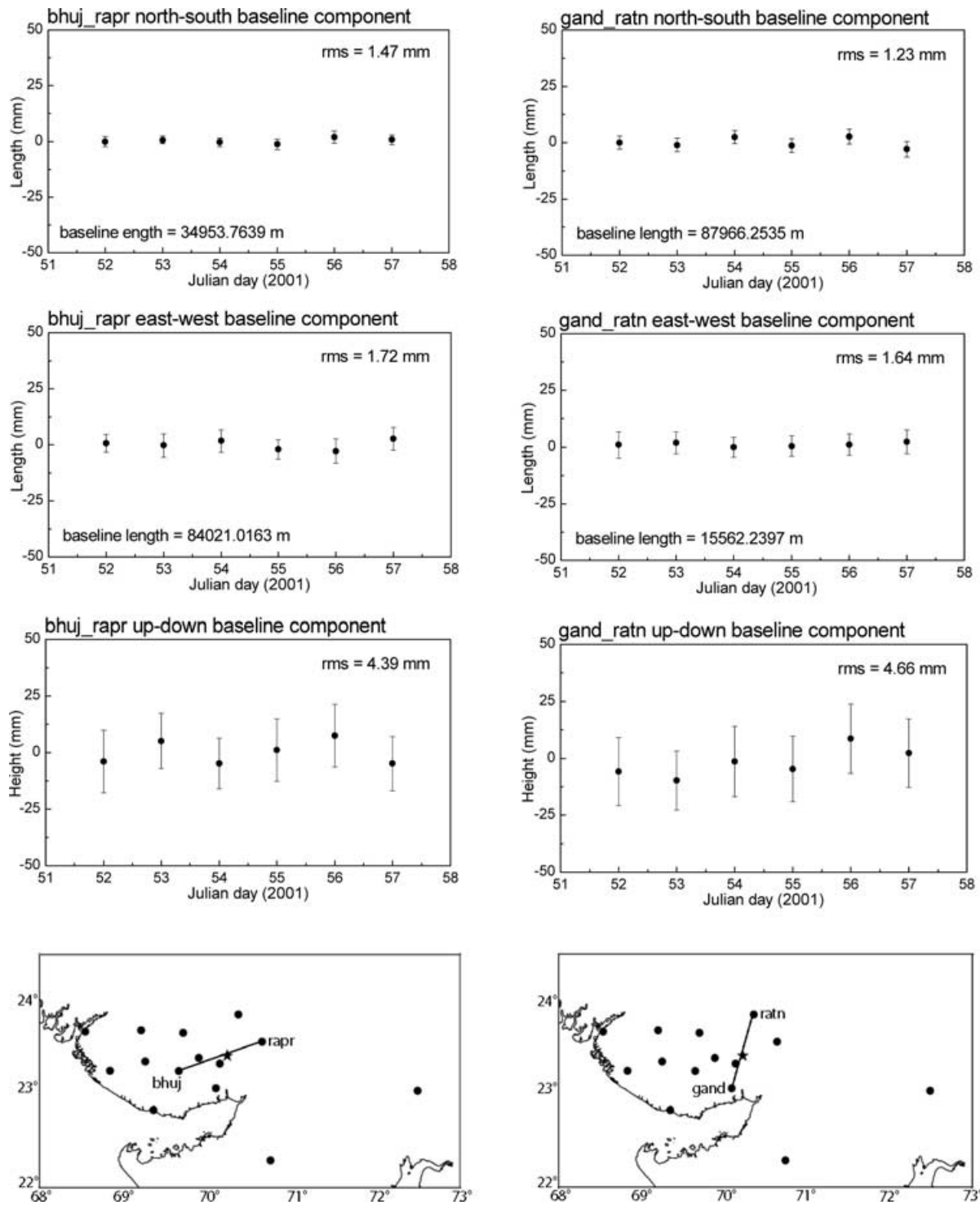
Figure 2. (*Continued.*)

Figure 3. North–south, east–west and up–down components of baselines passing though the epicentral area (a) BHUJ-RAPR baseline (as shown in left lower most block) (b) GAND-RATN baseline (as shown in the right lower most block) with their RMS value.

is concerned, the Bhuj region does not corroborate with the Kashmir and Andaman regions.

4 VELOCITY AND STRAIN DISTRIBUTION

The 2001–2002 velocity (in ITRF2000) has been derived at each site using GPS data from five campaigns. Table 1 and Fig. 4 give the velocity at all the sites along with the velocity vector of IGS station at Bangalore (IISC) shown in the inset of Fig. 4. The error ellipses (at the tip of the each velocity vector in Fig. 4) are drawn such that they give 95 per cent confidence level. The average velocity is found to be 50 ± 1.28 mm yr^{-1} towards NNE direction. The velocity distribution is more or less uniform over the entire study region except at the sites Dhamadkapir (DHAM) and Ratanpar (RATN), which portrayed anomalous velocity. The site DHAM exhibits a
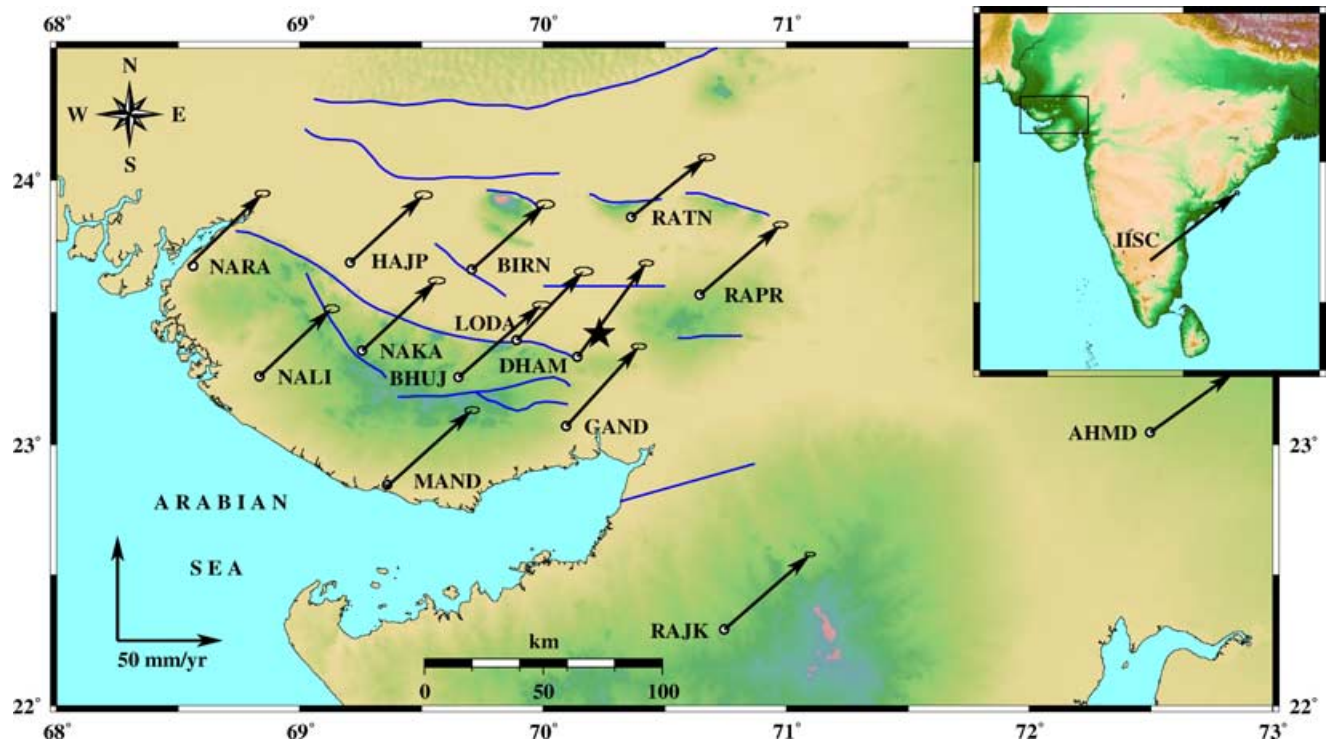
Figure 4. The velocity vectors with 95 per cent confidence error ellipses in ITRF2000 reference frame. The inset shows the velocity of IGS site IISC.

velocity of $44.64 \pm 0.60\,\text{mm}\,\text{yr}^{-1}$ in NS and $32.58 \pm 1.39\,\text{mm}\,\text{yr}^{-1}$ in EW horizontal components and the site RATN has a velocity of $28.60 \pm 0.60\,\text{mm}\,\text{yr}^{-1}$ in NS and $35.82 \pm 1.55\,\text{mm}\,\text{yr}^{-1}$ in EW components, respectively.

The time-series of the position coordinates are plotted in Figs 5(a) and (b). In general, the rms value estimated from all campaigns for each site shows, the north–south and east–west components are within the limit of ≥ 17.5 to $\leq 23.5\,\text{mm}$ and ≥ 19.5 to $\leq 22.5\,\text{mm}$, respectively with time-displacement variation following a linear trend. NS component of DHAM shows a high rms value of $25.04\,\text{mm}$ indicating possible post-seismic deformation in the fluid-filled fractured asperity zone (Kayal *et al.* 2002b). Since ITRF2000 is a conventional frame for global analysis, to realize the deformation activity in local scale, our GPS station velocities relative to fixed India are estimated and presented in Table 1 and Fig. 6. The residual velocity of the GPS sites in the India-fixed frame shows negligible post-seismic deformation in the western and eastern part of the epicentre. The change in velocity from DHAM ($11.62 \pm 1.51\,\text{yr}^{-1}$) in south to RATN ($5.24 \pm 1.69\,\text{mm}\,\text{yr}^{-1}$) in north cutting across the epicentral track suggests significant contractional deformation near the epicentre and confirms the convergence across the Kutch Rift Basin from the previous geodetic study reported by Jade *et al.* (2003).

The estimation of principal strain rate from the velocity field gives an average strain rate of contraction and extension of the order of 0.07 and 0.04 micro-strain yr^{-1}, respectively. However, principal strain towards the northern part of the epicentral region shows the highest compressional strain rate, that is, 0.30 micro-strain yr^{-1} with azimuth of $11°$ and the lowest extension rate, that is, 0.06 micro-strain yr^{-1} with azimuth of $101.25°$ (Fig. 6). To visualize accumulation of contractional strain in a better way, strain rate has been constructed along NS profile which is passing through the epicentral area (shown in Fig. 7) by plotting the contraction and extension strain components, and presented in Fig. 8. This clearly portrays

that within two years of the earthquake; significant contractional strain accumulation is going on towards the northern part of the epicentre.

To compare our result with seismological results, the seismic data were examined for eight major earthquakes and fault plane solutions of magnitude from 5.4 to 7.7 spanning the period 2001 January 26 to February 19 (Fig. 8). The analysis of this seismic data yielded only a general orientation for the principal stress axes, allowing only a qualitative comparison with the geodetic (GPS) results. The focal mechanism solution of the 2001 January 26 earthquake (Wesnousky *et al.* 2001; Negishi *et al.* 2002; Antolik & Dreger 2003) and the stress inversion performed from relocated aftershocks (Mandal *et al.* 2006) also consistently support the direction of north–south compression within the epicentral vicinity.

5 DISCUSSION

As far as the coseismic deformation associated with Bhuj earthquake is concerned, there is limited information, as no GPS sites were established in this region prior to the earthquake. However, based on GPS data during 1997–2001 from the site at Jamnagar which is ~108 km away from the epicentral region and GTS triangulation markers, Jade *et al.* (2003) and Wallace *et al.* (2006) measured coseismic deformation of $16 \pm 8\,\text{mm}$ at N35°E and very small post-seismic deformation. Analysis of satellite images (collected by Landsat, Terra, ERS and IRS-1D) near the epicentral region, before and after the earthquake shows a significant change in the flooding pattern of the Rann of Kutch due to coseismic uplift (Gahalaut & Burgmann 2004), however these data do not provide quantitative estimates on the coseismic deformation. Jade *et al.* (2003) and Wallace *et al.* (2006) report on estimates of coseismic deformation from resurveys of historic triangulation markers. Levelling and gravity measurements (Chandrasekhar *et al.* 2004) and interferometric
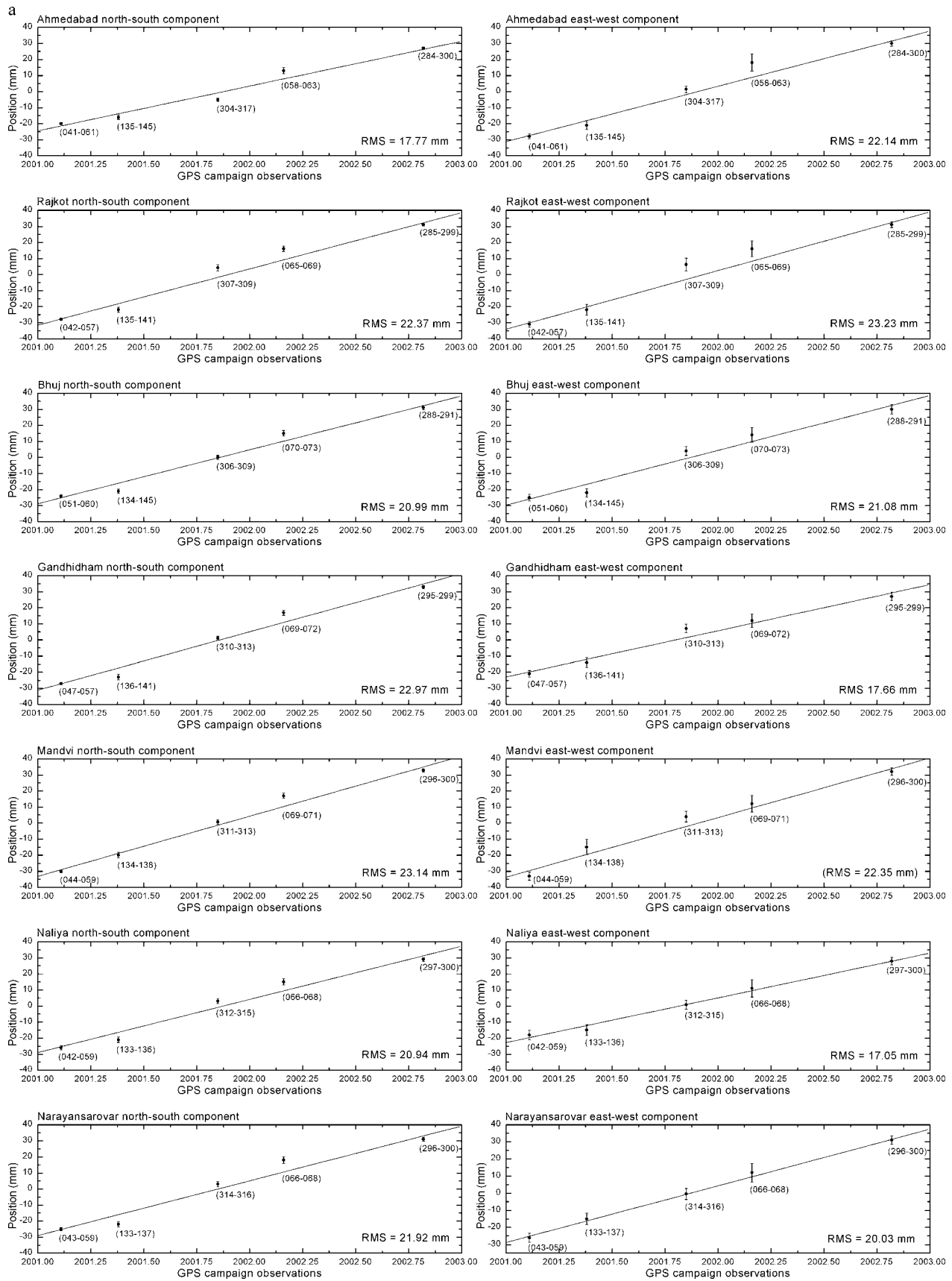
Figure 5. (a) Time-displacement variations at GPS sites AHMD, RAJK, BHUJ, GAND, MAND, NALI and NARA, from five GPS campaigns during 2001–2002. For each campaign, the single position is obtained by combining the covariance matrices for each day (the days of observations given in brackets). (b) Time-displacement variations at GPS sites NAKA, LODA, DHAM, RAPR, RATN, BIRN and HAP from five GPS campaigns during 2001–2002 (the days of observations given in brackets).
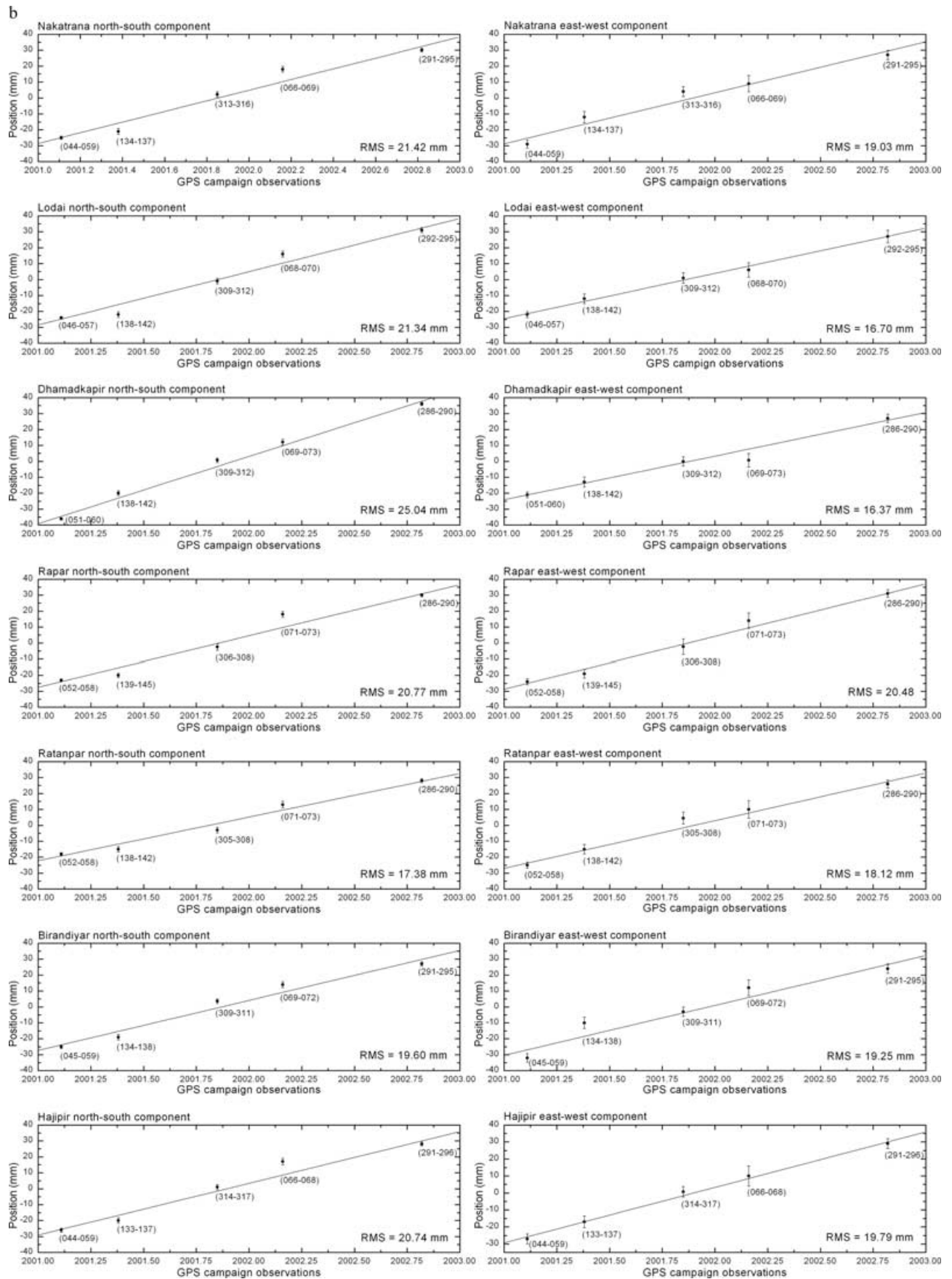
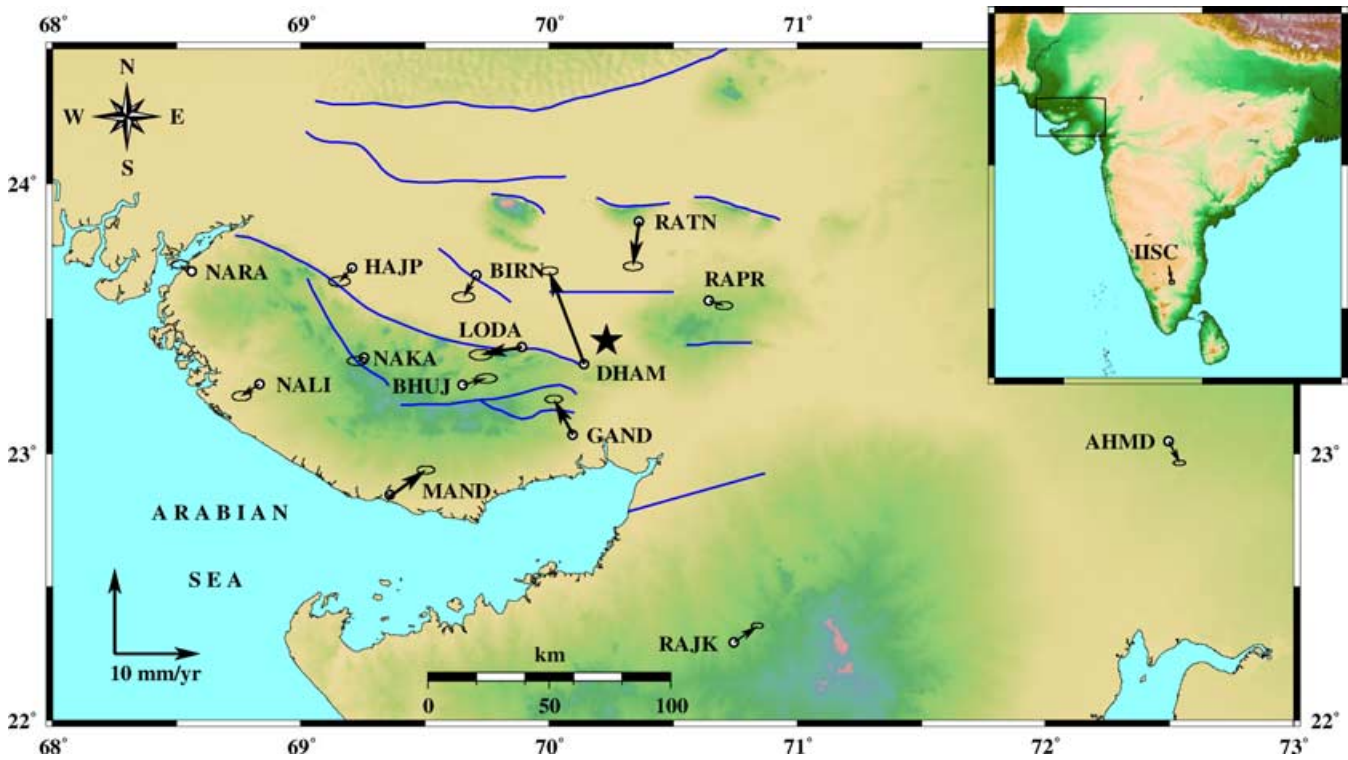**Figure 5.** (*Continued.*)

Figure 6. The velocity vectors with 95 per cent confidence error ellipses in India fixed reference frame. The inset shows the velocity of IGS site IISC.
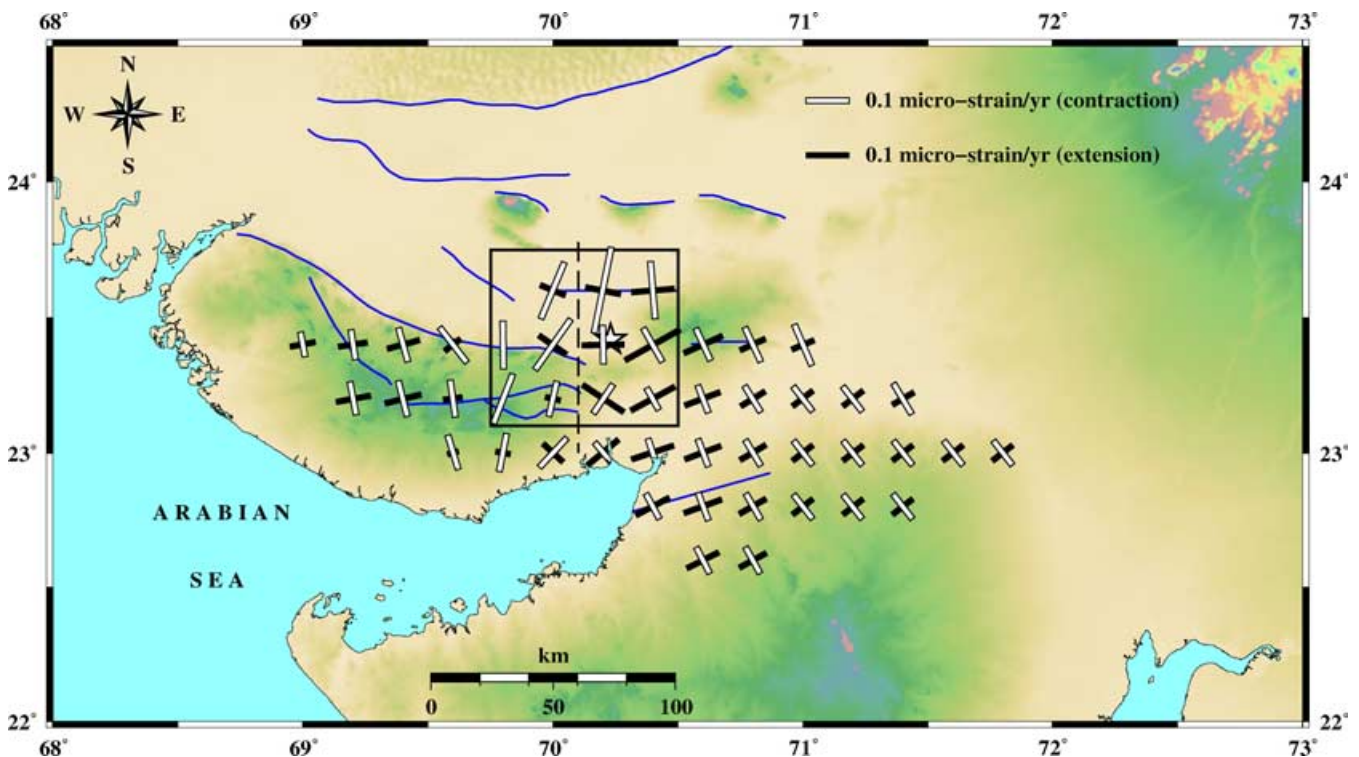

Figure 7. Principal strain rate axes computed from the GPS station velocities in ITRF2000. The rectangle shows the region of maximum compression. Dashed line indicates the line along which strain rate profile constructed (shown in Fig. 8).

synthetic aperture radar data (Schmidt & Burgmann 2006) provide further evidence that the rupture occurred on a deeply buried fault plane that is not clearly associated with any of the faults mapped at the surface.

The time-series of the site coordinates and baselines immediately after the earthquake (during 2001 February 10–March 2) indicate no detectable short-term post-seismic crustal deformation (Figs 2a and b). A single post-seismic interferogram provides an estimate of
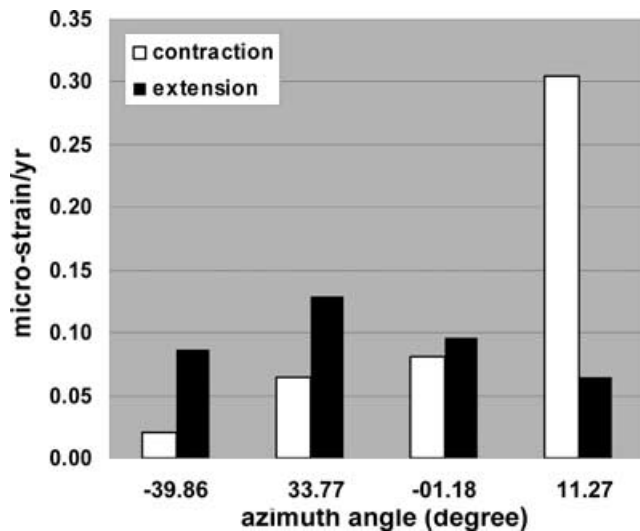
Figure 8. Strain rate profile (south–north, shown in Fig. 7) constructed by plotting the contraction and extension components.

range-change of less than ~5 mm (which is just above the inherent GPS error) (Schmidt & Burgmann 2006), which also implies that the short-term post-seismic deformation is small. Data from the five campaigns' horizontal components of displacement during 2001–2002 are well fit by linear trends (Figs 5a and b). None of the time-series clearly ensure either logarithmic or exponential functions implying any post-seismic relaxation from afterslip or viscoelasticity, which follows a slow decay. This small amount post-seismic relaxation might be due to the presence of the aseismic layer at 10–15 km depth (Kayal *et al.* 2002a), aseismic–seimic transition being sufficiently deep seated (To *et al.* 2004) and region of failed rift with blocks of basement rocks bounded by planar faults in the upper brittle crust of the study area (Biswas 2005).

The horizontal velocity fields with reference to ITRF2000 and in an Indian reference frame shown in Figs 4 and 6 provide new constraints on the kinematics of the western Indian region. The station velocities in ITRF2000 display the trend of all the sites in NNE direction at an average rate of 50 ± 1.28 mm yr^{-1} which is compatible with rates from other measurements in the Deccan trap region of western India as estimated by Reddy *et al.* (2000), that is, 51 mm yr^{-1} in N47°E. The pattern of the velocity components at the sites DHAM and RATN are anomalous compared to that of surrounding GPS sites (Fig. 4). When displayed with respect to the India-fixed frame (Fig. 6), the motion of the sites RATN and DHAM located on either north and south, respectively to the epicentre reveal a central compressional zone in north–south direction. This local compression is expected in the epicentral zone since it lies in the zone with a transpressional deformation at the eastern segment of KMF interacting with its transfer faults SWF (Biswas & Khattri 2002; Biswas 2005; Mathew *et al.* 2006) in the south and NWF (Mandal *et al.* 2004) to the north of the epicentre and due to the incipient or ongoing tectonic uplift of the Kutch mainland (Wallace *et al.* 2006). However, the trend of velocity at the GPS sites GAND and DHAM towards north–northwest and RATN towards south supports the left-lateral strike-slip movement (Kayal *et al.* 2002a) and the reverse fault movement of the south-dipping rupture fault plane (Wesnousky *et al.* 2001; Negishi *et al.* 2002; Antolik & Dreger 2003).

The estimated trend of the principal strain axes in this study near the epicentre shows north–south contraction and east–northeast to west–southwest extension (Fig. 7). A zone of maximum contrac-

tional strain is delineated towards the north epicentral area confined between the SWF (GPS site DHAM in Fig. 6) and NWF (demarcated by Mandal *et al.* 2004) regions (GPS site RATN in Fig. 6), with maximum contractional strain rate of 0.30 micro-strain yr^{-1}. These rates significantly exceed shortening rates across the Indian Peninsula of ~2–3 mm yr^{-1} that correspond to strain rates of only ~10^{-9} yr^{-1} (Paul *et al.* 2001). The axes of the principal strain displays the partitioning of contraction more or less perpendicular to the lineaments/faults system in the region, where as negligible amount of extension is noted along major fault systems in the region except some low amount near to the epicentre. The analysis of the north–south constructed strain profile (Fig. 8) cutting across the epicentre (Fig. 7) reveals an increasing trend of contractional strain rate from south to north and there is a sharp increase in the strain rate towards the northern part of the epicentre. On the other hand, the extension strain rate across the same profile shows the gently decreasing trend. The maximum extensions fall along the KHF in the west, KMF and SWF in south and east and NWF in the north of the epicentre. The strain field deduced from the GPS measurements is in agreement with the kinematics provided by the available earthquake focal mechanisms located towards the north of the epicentre (Fig. 9) and the stress inversion performed at different depths of the *P*- and *T*-axes of selected aftershocks suggest a dominant consistent north–south orientation of the *P*-axes over the aftershock zone (Mandal *et al.* 2006).

As other geophysical studies indicate, this region correlates with zone of magnetic sources such as of exposed volcanic rocks and subsurface intrusive bodies (Biswas 2005). Harinarain *et al.* (2003), from the analysis of the magnetotelluric (MT) studies delineated a 1–5 km depth of an undulating basement electrical structure across the Bhuj epicentral zone. This indicates a block structure in this region with different electrical conductivity character at deeper levels. The long period magnetotelluric (LMT) measurements in the period range of 10–6000 s have shown evidence of a crustal conductor in the depth range of 10–17 km, and a possible lithosphere-asthenosphere boundary at 150 km (IIG working group 2003). It is interesting to note that Bhuj earthquake with focus at 17 km depth was seated at the base of this high conductivity layer. The flow path of induced currents inferred from the nature of transient geomagnetic variations recorded from a 10-station magnetometer array also suggests the block crustal structure in the Kutch region. Such structures are often correlated with high seismic activity (Arora & Reddy 2001). Mandal *et al.* (2004), from their *Vp* and *Vp*/*Vs* tomographic results suggest the presence of an ultramafic body characterized by high V and low σ at 10–40 km depths beneath the epicentral zone resting on the base of the lower crust. This high velocity bell-shaped body exists in most of the 160 km × 160 km area of Kutch at the bottom and 40 km × 30 km at the top. It must be contributing significantly in inducing large crustal stresses resulting in the generation of great earthquakes in this intraplate area similar to the mechanism suggested by Pollitz *et al.* (2002). The high-*Vp*, low-*Vs* and high Poisson's ratio (σ) from the 3-D seismic velocity (Kayal *et al.* 2002b) and high scatter in shear wave time delays indicates (Padhy & Crampin 2005) the presence of fluid filled fractured rock matrix in the source zone and pore-fluid pressure on all seismogenic faults, respectively.

A viscoelastic model with internal rheologic heterogeneities developed by Qingsong *et al.* (2002) indicates intracontinental thrusting and shearing, and predicts a broad earthquake prone zone. With a high velocity and large conductive mass of the mafic intrusive body extending to the lower crust (Mandal *et al.* 2004), basement controlled by numerous thrust faults (Mishra *et al.* 2005), the
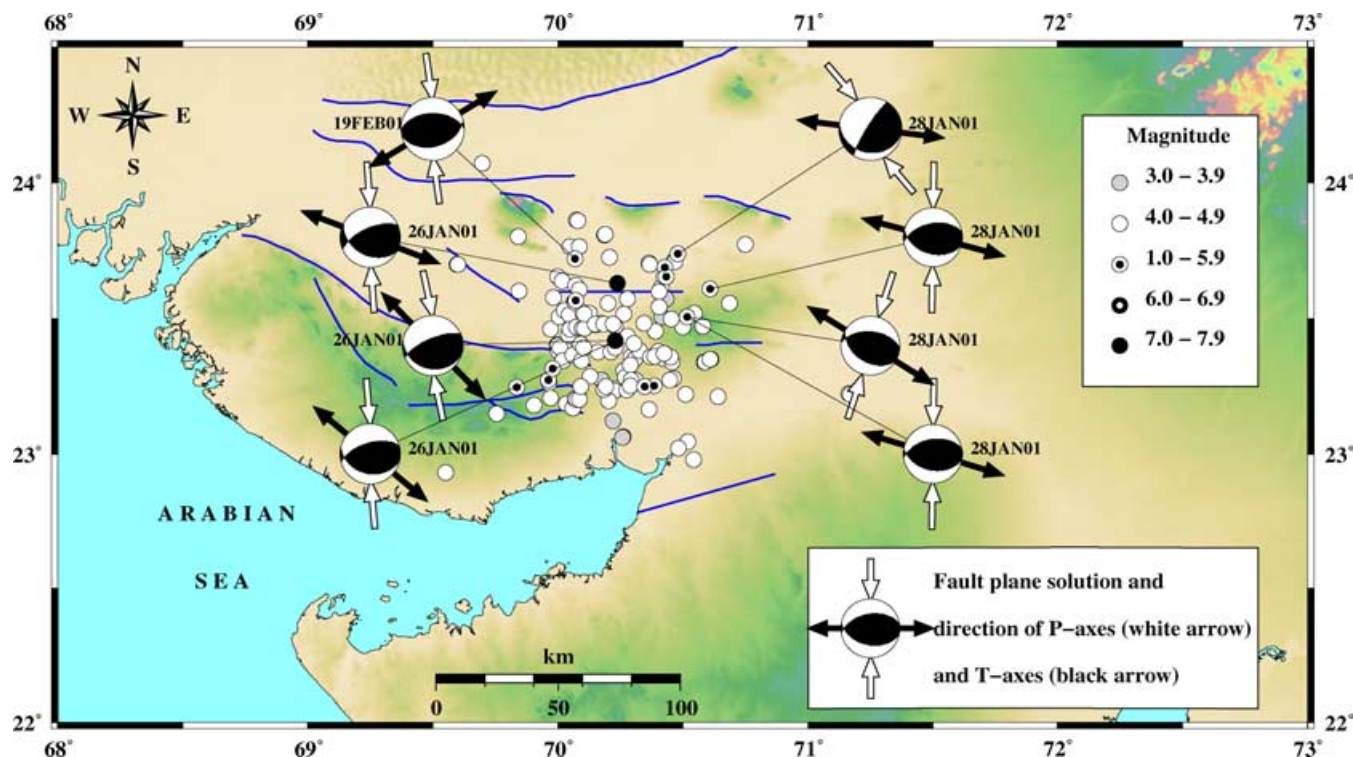
Figure 9. Focal mechanism solutions with *P*- and *T*-axes obtained from National Earthquake Information Centre (NEIC) with the date of occurrence of the events. The small circles indicate the spatial distribution of the aftershocks with different magnitudes.

location of the causative fault for Bhuj earthquake at the depth of 9–10 km with in the basement (Negishi *et al.* 2002; Chandrasekhar *et al.* 2004) with large slip in the shallow part (Antolik & Dreger 2003) are making their contribution for local compressive regime indicated in Fig. 7. Kayal *et al.* (2002a) inferred that the intersection of two faults (KMF and SWF) has been the source area for stress accumulation. Ravi Sankar (1995) suggests that the differential thermal and crustal structure provide the first order force for the relative movement between the sites DHAM and RATN (Fig. 6). From the velocity structure obtained from eight broadband stations in Kutch basin and Saurashtra areas, Mandal (2006) suggests that generation of the stress required to cause the Bhuj earthquake is due to the Moho upwarping beneath the epicentral zone. Many geophysical studies support the Bhuj earthquake of January 2001 and following post seismic activity is analogous to 1811-12 intraplate earthquakes (M_w 7.8) such as those in the New Madrid seismic zone in Central United states (Newman *et al.* 1999; Qingsong *et al.* 2005; Smalley *et al.* 2005; Tuttle 2005). From continuous GPS measurements, the indicated strain rate of 10^{-7} yr^{-1} in New Madrid region is much less than the estimated strain rate in Bhuj region.

The deformation of the GPS sites DHAM (south) and RATN (north) and the strain partitioning in this study pointing towards the presence of a deep block structure between the SWF and NWF and the evidence from geological, geophysical and geodetics studies are consistent in identifying a region of significant compression demarcated in Fig. 7. The nucleation at middle lower crust makes it difficult to delineate the main force of compressive stress. Still the highest observed strain rate and the recurrence of moderate earthquakes [on 2003 August 5 (M_w 5.0) and 2006 March 7 (M_w 5.2)] with epicentres located (given by USGS) towards the north–northeast of the Bhuj earthquake region gives information that the presence of ongoing activity of the strain accumulation due to the localized

driving force in the region. Further, the convergent strain across the south-dipping reverse earthquakes on the Kutch mainland suggests the contribution of the present neo-tectonic NNE–SSW compressive stress regime of the Indian Plate. The continued northerly ridge push from the Carlsberg Ridge against the collision front in the north, its proximity to the India, Arabia, Asia triple junction in the western continental margin, the readjustment of the crust associated with the main shock, and the nature of existing fault system (Biswas 1987; Gowd *et al.* 1996; Biswas & Khatri 2002) collectively contribute to the anomaly in strain rate.

6 CONCLUSION

After the 2001 January 26 Bhuj earthquake, five GPS campaigns were carried out during 2001–2002, at 14 sites. Early transient (short-term) post seismic relaxation was not conspicuous during 2001 February 21 to March 2. The displacement time-series over two years duration also did not prominently show characteristics of post-seismic relaxation due to afterslip, visco and poro elasticity. The velocity field with reference to ITRF2000 and Indian Plate fixed frame clearly portrays NS contraction between the sites DHAM and RATN, which are located on either side of the epicentral track region. A maximum contractional strain rate of about 0.30 micro-strain yr^{-1} was observed in this region. All geophysical studies carried out in this region showed anomalous behaviour, consistent in delineating this region as a compressive regime with a block structure between the SWF and NWF. Our results also are fairly consistent with a number of features documented in previous geological, geophysical and geodetic studies. The scenario in Bhuj region with ongoing compression and high strain rate may indicate a high risk of another earthquake in the Kutch rift basin. Continued

GPS measurements and InSAR data acquisitions may provide post seismic transients and spatial deformation. Viscoelastic modelling of this region would help to describe the post-seismic response and stress state of the lithosphere.

REFERENCES

Altamimi, Z., Sillard, P. & Boucher, C., 2002. ITRF2000: a new release of the International Terrestrial Reference Frame for earth science applications, *J. geophys. Res.,* **107**(B10) doi:10.1029/2001JB000561.

Antolik, M. & Dreger, D.S., 2003. Rupture of the January 2001Mw 7.6 Bhuj, India, earthquake from teleseismic broadband data, *Bull. seism. Soc. Am.,* **93**(3) 1235–1248.

Arora, B.R. & Reddy, C.D., 2001. Correlation between high electrical conductivity and seismicity: role of fluids, *Ind. Geol. Congress,* **1,** 267–276.

Arya, A.S., 2000. Recent developments towards earthquake risk reduction in India, *Curr. Sci.,* **79,** 1270–1277.

Bendick, R. *et al.*, 2001. The 26 January 2001 "Republic Day" earthquake, India, *Seism. Res. Lett.,* **72**(3) 328–335.

Bilham, R., 1999. Coastal Tectonics, in *Geol. Soc. London.,* Vol. 146, pp. 295–318, eds Stewart, I.S. & Vita-Finzi, The Geological Society, London.

Biswas, S.K., 1987. Regional tectonic framework, structure and evolution of the western marginal basins of India, *Tectonophysics,* **135,** 307–327.

Biswas, S.K., 2005. A review of structure and tectonics of Kutch basin, western India, with special reference to earthquakes, *Curr. Sci.,* **88**(10) 1592–1600.

Biswas, S.K. & Khattri, K.N., 2002. A Geological study of Earthquakes in Kutch, Gujarat, India, *J. Geol. Soc. India,* **60**(2) 131–142.

Chandrasekhar, D.V., Mishra, D.C., Sigh, B., Kumar, V. & Bürgmann, R., 2004. Source parameters of the Bhuj earthquake, India of January 26, 2001 from height and gravity changes, *Geophys. Res. Lett.,* **31,** GL020768.

Chen, Z. *et al.*, 2000. Global Positioning System measurements from eastern Tibet and their implications for India/Eurasia intercontinental deformation, *J. geophys. Res.,* **105**(B7) 16 215–16 228, doi:10.1029/2000JB900092.

Chung, W.Y. & Gao, H., 1995. Source parameters of the Anjar earthquake of July 21, 1956, India, and its seismotectonic implications for the Kutch rift basin, *Tectonophysics,* **242,** 281–292.

Dong, D., Herring, T.A & King, R.W., 1998. Estimating regional from a combination of space and terrestrial gedetic data, *J. Geod.,* **72,** 200–214.

Feigl., K.L., King, R.W. & Jordan, T.H., 1990. Geodetic measurement of tectonic deformation in the Santa Maria Fold and Thrust Belt, California, *J. geophys. Res.,* **90,** 2679–2699.

Gahalaut, V. & Bürgmann, R., 2004. Constrain on the source parameters of the 26 January 2001Bhuj, India, earthquake from satellite images, *Bull. seism. Soc. Am.,* **94**(6) 2407–2413.

Gowd, T.N, Srirama Rao, S.V. & Chary, K.B., 1996. Stress field and seismicity in the Indian shield: effects of the collision between India and Eurasia, *Pageoph,* **146,** 503–531.

Harinarayana, T., Patro, B.P.K., Naganjaneyulu, K., Begun, S.K. & Virupakshi, G., 2003. Deep electrical structure across the Bhuj earthquake epicentral zone, India, *Seismic and Volcanic Studies, Session EM9–1,* Sapporo, Japan.

Herring, T.A., 2000. GLOBK: global Kalman filter VLBI and GPS analysis programme version 10.0, Massachusetts Institute of Technology, Cambridge.

Herring, T.A., Davis, J.L. & Shapiro, 1990. Geodesy by radio interferometry: the application of Kalman filtering to the analysis of very long baseline interferometry data, *J. geophys. Res.,* **95,** 12 561–12 581,

IIG working group for Bhuj Earthquake Related studies (Arora *et al.* Mita Rajaram *et al.* C.D. Reddy *et al.*), 2001. Geophysical investigations in the January 26, 2001 Bhuj earthquake affected region, *Workshop on Recent Earthquakes of Chamoli and Bhuj,* May 24–26.

Jade, S. *et al.*, 2003. Pre-Seismic, Co-seismic and post-seismic displacement associated with the Bhjuj 2001 earthquake derived from recent historic geodetic data, *Proc. Indian Acad. Sci. Earth Planet Sci.,* **112,** 331–345.

Karant, R.V., 2001. Neotectonics and Paleoseismicity of Kachchh, Western India, Research Highlights in Earth System Science, *DST's spl. Vol. 2 on "Seismicity",* pp. 159–179, ed. Varma, O.P., Indian Geological Congress.

Kayal, J.R., Reena, De, Sagina, Ram, Srirama, B.V. & Gaonkar, S.G., 2002a. Aftershocks of the 26 January, 2001 Bhuj earthquake in western India and its seismotectonic implications, *J. Geol. Soc. India,* **59,** 395–417.

Kayal, J.R., Zaho, D., Mishra, O.P., De, R. & Singh, O.P., 2002b. The 2001 Bhuj earthquake: tomographic evidence for fluids at the hypocenter and its implications for rupture nucleation, *Geophys. Res. Lett.,* **29**(24) doi:10.1029/2002GL015177.

King, R.W. & Bock, Y., 2000. GAMIT: documentation for GMIT GPS Analysis Software, Version 10.01, *Massachusetts Institute of Technology and Scripps Institution of Oceanography*, Cambridge.

Malik, J.N., Sohoni, P.S., Merh, S.S. & Karanth, R.V., 2000. Palaeoseismology and neotectonism of Kachchh, Western India, in *Active Fault Research for new Millenium*, Proceedings of the Hokudan International Symposium and School on Active Faulting, pp. 251–259, eds Okumura, K., Takada, K. & Goto, H., Proceedings of the tbkudan International Symposium and School on Active Faulting, Japan.

Mandal, P., 2006. Sedimentary and crustal structure beneath Kachchh and Saurashtra regions, Gujarat, India, *Phys. Earth Plan. Int.,* **155,** 286–299.

Mandal, P., Horton, S. & Pujol, J., 2006. Relocation, Vp and Vp/Vs tomography, focal mechanisms and other related studies using aftershock data of the Mw 7.7 Bhuj earthquake of January 26, 2002, *J. Ind. geophys. Union,* **10,** 31–44.

Mandal, P. *et al.*, 2004. Characterization of the causative fault system for 2001 Bhuj earthquake of Mw 7.7, *Tectonophysics,* **378,** 105–121.

Mathew, G., Singhvi, A.K. & Karanth, R.V., 2006. Luminescence chronometry and geomorphic evidence of active fold growth along the Kachchh Mainland Fault (KMF), Kachchh, India: seismotectonic implications, *Tectonophysics,* **422,** 71–87.

McClusky, S. *et al*., 2000. Global Positioning System constraints on plate kinematics and dynamics in the eastern Mediterranean and Caucasus, *J. geophys. Res.,* **105**(B3) 5695–5720, 10.1029/1999JB900351, 2000.

Mishra, D.C., Chandrasekhar, D.V. & Singh, B., 2005. Tectonics and crustal structures to Bhuj earthquake of January 26, 2001: based on gravity and magnetic surveys constrained from seismic and seismological studies, *Tectonophysics,* **396,** 195–207.

Miura, S., Suwa, Y., Sato, T., Tachibana, K. & Hasegawa, A., 2004. Slip distribution of the 2003 northern Miyagi earthquake (M6.4) deduced from geodetic inversion, *Earth Planet Space,* **56,** 95–101.

Negishi, H., Mori, J., Sato, T., Singh, R., Kumar, S. & Hirata, N., 2002. Size and orientation of the fault plane for the 2001 Gujarat, India earthquake (Mw 7.7) from aftershock observations: a high stress drop event, *Geophys. Res. Lett.,* **29**(20) GL015280.

Newman, A., Stein, S., Weber, J., Englen, J., Mao, A. & Dixon, T., 1999. Slow deformation and lower seismic hazard at new Madrid seismic zone, *Science,* **284,** 619–621.

Padhy, S. & Crampin, S., 2005. High pore-fluid pressures at Bhuj, inferred from 90°–filps in shear-wave polarizations, *Gephys. J. Int.,* **164,** 370–376.

Parsons, T., Yeats, R.S., Yagi, Y. & Hussain, A., 2006. Static stress change from the 8 October, 2005 M = 7.6 Kashmir earthquake, *Geophys. Res. Lett.,* **33,** L06304, doi:10.1029/2005GL025429.

Paul, J. *et al.*, 2001. The motion of and active deformation of India, *Geophys. Res. Lett.,* **28**(4) 647–650.

Peltzer, G., Rosen, P., Rogez, F. & Hudnut, K., 1998. Poroelastic rebound along the Landers 1992 earthquake surface rupture, *J. geophys. Res.,* **103,** 30 131–30 145.

Pollitz, F.F., 2003. Postseismic relaxation theory on a laterally heterogeneous viscoelastic model. *Geophys. J. Int.,* **155,** 57–78.

Pollitz F, Kellogg L. & Bürgmann, R., 2002. Sinking mafic body in a re-activated lower crust: a mechanism for stress concentration in the New Madrid Seismic Zone. *Bull. seism. Soc. Am.* **91,** 1882–1897.

Pollitz, F.F., Bürgmann, R. & Banerjee, P., 2006. Post-seismic relaxation following the great 2004 Sumatra-Andaman earthquake on a compressible self-gravitating Earth, *Geophys. J. Int.,* **167,** 397–420.

Qingsong, Li, Liu M. & Yang, Y., 2002. The 01/26/2001, Bhuj, India earthquake: intraplate or interplate? *Plate Boundary Zone,* pp. 255–264, eds Stein, S.. & Freymueller, J., AGU, Washington, DC.

Qingsong, Li, Liu M. & Sandvol, E., 2005. Stress evolution following the 1811-1812 large earthquake in the New Madrid seismic zone, *Geophys. Res. Lett.,* **32,** GL011310.

Rajendran, C.P. & Rajendran, K., 2001. Characteristics of deformation and past seismicity associated with the 1819 Kutch earthquake, Nortwestern India, *Bull. seism. Soc. Am.,* **91,** 407–426.

Ravi Sankar, 1995. Fragmented Indian shield and recent earthquakes, *Geol. Surv. India Spec. Publ.,* **27,** 41–48.

Reddy, C.D. & Prajapati, S.K., 2007. GPS measurement of the post-seismic deformation due to 8th October 2005 Kashmir Earthquake, in the devasting Muzaffrabad earthquake of 8th October 2005 in Western Himalaya Gupta *et al.* ed., *J. Seismol.* in press.

Reddy, C.D., El-Fiky, G., Kato, T., Shimada, S. & Kumar, V., 2000. Crustal strain field in the Deccan trap region, western India, derived from GPS measurements, *Earth Planet Space,* **52,** 965–969.

Reddy, C.D., Prajapati, S.K. & Kato, T., 2005.Characteristics of Post-seismic relaxation in Andaman-Nicobar region from continuous GPS measurements, *Proceedings of the International Workshop on the Restoration Program from Giant Earthquake and Tsunamis,* **Part 1**, 91–95.

Scherneck, H.G., Jan, M., Jahonsson, Vermeer, M., James, L.D., Glenn, A.M. & Jerry, M. M, 2001. BIFROST Project: 3-D crustal deformation rates derived from GPS confirm post glacial rebound in Fennoscandia, *Earth Planet Space,* **53,** 703–708.

Schmidt, D.A. & Burgmann, R., 2006. InSAR constrains on the source parameters of the 2001 Bhuj earthquake, *Geophys. Res. Lett.,* **33,** L02315.

Smalley, R. Jr., Ellis, M.A., Paul, J. & Arsdale, V., 2005. Space geodetic evidence for rapid strain rates in the New Madrid seismic zone of central USA, *Nature,* **435,** 1088–1090.

Socquet, A., Vigny, C., Chamot-Rooke, N., Simons, W., Rangin, C. & Ambrosius, B., 2006. India and Sunda plates motion and deformation along their boundary in Myanmar determined by GPS, *J. geophys. Res.,* **111,** B05406, doi:10.1029/2005JB003877.

To, A., Burgmann, R. & Pollitz, F., 2004. Postseismic deformation and stress changes following the 1819 Rann of Kachchh, India earthquake: was the 2001 Bhuj earthquake a triggered even?, *Geophys. Res. Lett.,* **31,** L13609.

Tuttle, M.P., 2005. New Madrid in motion, *Nature,* **435,** 1037–1039.

Wallace, K., Bilham, R., Blume, F., Gaur, V.K. & Gahalaut, V., 2006. Geodetic constrains on the Bhuj 2001 earthquake and surface deformation in the Kachchh Rift Basin, *Gephys. Res. Lett.,* **33,** L10301, doi:10.1029/2006GL025775.

Wesnousky, S.G., Seeber, L., Rockwell, T.K., Thakur, V., Briggs, R., Kumar, S. & Ragona, D., 2001, *Seism. Res. Lett.,* **72,** 514–524.